Multishell contribution to the Dzyaloshinskii-Moriya spiraling in MnSi-type crystals

Viacheslav A. Chizhikov* and Vladimir E. Dmitrienko†
A.V. Shubnikov Institute of Crystallography, 119333 Moscow, Russia
(Received 8 April 2013; revised manuscript received 26 August 2013; published 3 December 2013)

The transition from the microscopic Heisenberg model to the macroscopic elastic theory is carried out for MnSi-type chiral magnetics with $B20$ crystal structure. Both exchange and Dzyaloshinskii-Moriya (DM) interactions are taken into account for the first, second, and third magnetic neighbors. The particular components of the DM vectors of bonds are found, which are responsible for (i) the global magnetic twist and (ii) the canting between four different spin sublattices. A possible mechanism for effective reinforcement of the global magnetic twist is suggested: it is demonstrated that the components of the DM vectors normal to corresponding interatomic bonds become very important for the twisting power. The Ruderman-Kittel-Kasuya-Yosida (RKKY) theory is used for model calculation of exchange parameters. It is found that just the interplay between the exchange parameters of several magnetic shells rather than the signs of DM vectors can be responsible for the concentration-induced reverse of the magnetic chirality recently observed in $Mn_{1-x}Fe_xGe$ crystals.

DOI: 10.1103/PhysRevB.88.214402 PACS number(s): 75.25.−j, 75.10.Hk

I. INTRODUCTION

Chiral spin textures are studied now very actively for possible spin self-organization, unusual quantum transport phenomena, and spintronic applications. A well established mechanism of spin chirality is the spin-orbit Dzyaloshinskii-Moriya (DM) interaction which is responsible for intricate magnetic patterns in MnSi-type crystals. Even half a century after the discovery of the strange magnetic properties of MnSi,[1,2] the magnetics of the $B20$ crystal structure still amaze us with the variety and complexity of their magnetic phases and electronic properties,[3] contrasting with the simplicity of the crystalline arrangement (only four magnetic atoms per unit cell). Among the magnetic phases, both experimentally observed and hypothetical, are simple and cone helices,[4,5] the Skyrmions and their lattices associated with the recently found A phase,[6–9] possible three-dimensional (3D) structures[10–12] similar to the blue phases of liquid crystals, etc. This variety is due to, first, the lack of inverse and mirror symmetries, which gives rise to the chirality of the crystalline and spin structures; second, the frustrations[13,14] resulting from the nontrivial topology of the trillium lattice, that introduces a competition of various interactions between different pairs of atoms.

Beginning from the discovery of the chiral magnetic properties of MnSi in 1976[4,5] till the present day, the most used approach to describe and predict twisted magnetic structures remains the phenomenological theory based on the Ginsburg-Landau free energy with an additional term first introduced by Dzyaloshinskii.[10,11,15–17] However, the approach, which uses our knowledge of the system symmetry, is not able to say anything about the values of coefficients in the free energy; for instance, how they are connected with the real interactions between atoms.

The microscopic theories, e.g., the model of classical Heisenberg ferromagnetics with a spin-orbit term originally developed by Moriya,[18] have in their turn the shortcoming that the number of variables, including the spins of all the magnetic atoms, is infinite, and therefore they are difficult to use for any analytical computations. Nevertheless, in spite of some doubts about the validity of the Heisenberg model in the itinerant magnetics, it is often used for digital simulations.[12,19] For this model it is of great importance to know the parameters of different interactions between pairs of spins: J_{ij} for the exchange coupling of the ith and jth atoms, and vectors $\mathbf{D}_{ij}$ for DM interactions. Those parameters can be obtained in two ways: from comparison of theoretical results with an experimental data and by means of *ab intio* calculations.

In our recent work,[14] using a coarse-grained approximation, the phenomenological constants $\mathcal{J}$ and $\mathcal{D}$ of the elastic free energy have been connected with the corresponding parameters of the microscopic theory. A surprising detail was the recognition of intersublattice canting as a new microscopic feature of the magnetic structures in MnSi-type crystals. Figure 1 shows the difference between the twist and the canting by example of a 1D spin chain. An experimental confirmation of the canting could give us an argument for applicability of the Heisenberg model to MnSi-type itinerant ferromagnetics.[20] Similar features could be observed in dielectric chiral magnetics, such as in the recently studied multiferroics Cu_2OSeO_3,[21–23] $BiFeO_3$[24] and in langasite-type crystals.[25]

Though the theory with only nearest-neighbors interactions is frequently used to simulate spin structures,[12,14,19] it does not always give an adequate physical description. Thus, as we discuss in the next section, the nearest-neighbors approximation needs abnormally strong spin-orbit interaction in order to describe helical and Skyrmion states in some $B20$ structures, e.g., in MnGe. Besides, very often the coupling between second and next neighbors is comparable or even more considerable than that of the nearest neighbors. Thus, for example, in the weak ferromagnetic α-Fe_2O_3, the antiferromagnetic exchange interactions and DM interactions are expected to be the most strong for third and fourth neighbors (see *ab initio* calculations in Ref. 26); this is also supported by the experimental data for the Heisenberg exchange parameters.[27]

It also could happen that only with the interactions between non-nearest neighbors can one describe an experimentally observed phenomenon. For example, if in a 1D spin chain with ferromagnetic coupling between the nearest neighbors

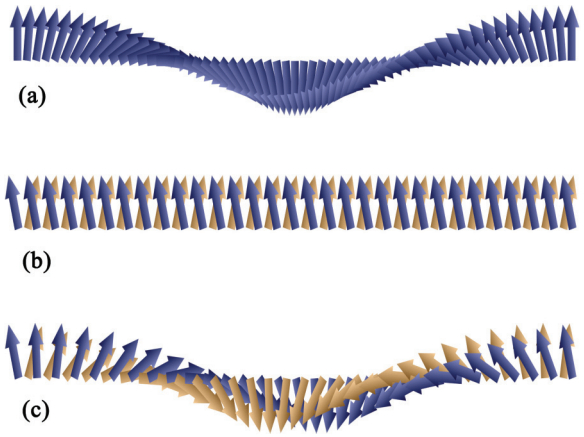

FIG. 1. (Color online) (a) The 1D twisted magnetic structure; the spins rotate in the plane perpendicular to the propagation vector. (b) The canting in the absence of a twist; the lattice is divided into two sublattices (blue- and sand-colored arrows) with the spins tilted by a constant angle. (c) The canting and the twist; the canting of the sublattices leads to the combination of two helices with the same propagation vector and a constant phase shift.

($J_1 > 0$) one turns on the antiferromagnetic interaction with the second neighbors ($J_2 < 0$), then for $|J_2| > J_1/4$ a spiral magnetic structure appears owing to spontaneous breaking of the inverse symmetry. Such approach can explain the phase transition appearing at ∼28 K and inducing ferroelectricity in the multiferroic Tb(Dy)MnO_3 crystal.[28,29] The approach works also in the MnSi-type itinerant magnetics. Just the competition between ferromagnetic coupling of the nearest spins ($J_1 > 0$) and antiferromagnetic coupling of the second and third neighbors ($J_2 \approx J_3 < 0$) was utilized to explain the observed alignment of magnetic helices along crystallographic directions ⟨110⟩ in MnSi at high pressure.[30]

In this paper, we suggest a possible mechanism for effective reinforcement of the twist terms in the chiral spin structures of the $B20$ magnetics, taking into account the interactions with non-nearest neighbors. The reinforcement is caused by an interplay between the exchange coupling with the second and third neighbors and the canting from DM interactions. In Secs. II–VI the transition from the Heisenberg microscopic model to the continuous phenomenological one is performed, and the spin-orbit terms in the phenomenological energy are found up to contributions of the order of $(D/J)^2$. In Sec. VII the possibility of an extra twist induced by the canting is demonstrated. In Sec. VIII the exchange interaction parameters are estimated within the Ruderman-Kittel-Kasuya-Yosida (RKKY) theory. In Sec. IX the possibility of an experimental proof of the canting existence is discussed. The possible applications of the theory are suggested in Sec. X.

II. DZYALOSHINSKII-MORIYA INTERACTION IN MICROSCOPICAL AND PHENOMENOLOGICAL APPROACHES

Both phenomenological and microscopical theories describing twisted MnSi-type magnetics contain terms induced by chirality of the system and associated with the Dzyaloshinskii-Moriya interaction of the spin-orbit nature. In the Heisenberg model, the extra term being associated with an individual bond, e.g., connecting magnetic atoms 1 and 2, can be expressed as

$$\mathbf{D}_{12} \cdot [\mathbf{s}_1 \times \mathbf{s}_2], \tag{1}$$

where $\mathbf{s}_1$ and $\mathbf{s}_2$ are the classical spins of the atoms, $\mathbf{D}_{12}$ is the DM vector of the bond 1-2. In principle, there could be magnetic moments at Si atoms[31] but this effect will be neglected below. Let us briefly describe the properties of the DM vector.[18] (i) As is obvious from Eq. (1), the sign of the DM vector depends on which atom of the bond we consider as the first. Indeed, because the cross product changes its sign when $\mathbf{s}_1$ and $\mathbf{s}_2$ are rearranged, then $\mathbf{D}_{21} = -\mathbf{D}_{12}$. (ii) The structure changes its chirality under inversion, whereas the energy remains unchanged, which means that $\mathbf{D}_{12}$ is a pseudovector, because $[\mathbf{s}_1 \times \mathbf{s}_2]$ is a pseudovector as well. (iii) The DM vector of a bond possesses the local symmetry of the bond. Thus, in MnSi the DM vectors are of their most general form; i.e., they have three independent components, because the Mn-Mn bonds in the $B20$ structure do not possess any internal symmetry element. (iv) The DM vectors vary from bond to bond; the DM vectors of the equivalent bonds have the same length but may be of different orientation (just the case of MnSi). In particular, if two bonds are connected by the rotation symmetry transformation of the space group $P2_13$ of the crystal, then their DM vectors are connected by the corresponding rotation of the point group 23.

In phenomenological theory, the chiral interaction is induced by the extra term

$$\mathcal{D}\mathbf{M} \cdot [\nabla \times \mathbf{M}] \tag{2}$$

in the expression for the magnetic energy density. Here $\mathbf{M}$ is a continuous field of the magnetic moment, and $\mathcal{D}$ is a pseudoscalar constant of the interaction.

Because both the theories describe the same matter, there should be a relationship between them. In particular, the terms (1) and (2) of the different approaches should be somehow connected. Indeed, it was shown in Ref. 14 that in the nearest-neighbors approximation the constant $\mathcal{D}$ of the phenomenological theory is proportional to the component $(D_x - 2D_y - D_z)$ of the DM vector of the bond $(-2x, \frac{1}{2}, \frac{1}{2} - 2x)$ between neighboring manganese atoms.

However, there is a problem here. According to different spin-orbit calculation schemes,[26,29,32–35] the DM vector associated with a bond should be perpendicular or almost perpendicular to the bond. In the present case it means that the component $(D_x - 2D_y - D_z)$, which lies almost along the bond, constitutes only a small part of the DM vector length. Taking into account that having the relativistic nature spin-orbit DM interaction serves as a small additive to the ferromagnetic exchange coupling, we can conclude that the twist observed in the MnSi-type crystals, particularly in MnGe, seems to be abnormally strong. A possible solution of this problem is that the nearest-neighbors approximation is not sufficient and hereinafter we develop this idea in detail.

In the following sections we will show, how to perform transformation from the microscopic Heisenberg model to the macroscopic elastic theory.

III. FROM THE HEISENBERG MODEL TO A CONTINUOUS APPROXIMATION

In the classical Heisenberg model of magnetics with an extra interaction of the Dzyaloshinskii-Moriya type, the energy of the system is expressed as a sum of pair interactions between magnetic atoms and the interaction of individual atoms with an external magnetic field $\mathbf{H}$:

$$E = \sum_{\text{cells}} \left(\sum_{n,\{ij\}} \left\{ -\tilde{J}_n \mathbf{s}_i \cdot \mathbf{s}_j + \mathbf{D}_{n,ij} \cdot [\mathbf{s}_i \times \mathbf{s}_j] - \frac{(\mathbf{D}_{n,ij} \cdot \mathbf{s}_i)(\mathbf{D}_{n,ij} \cdot \mathbf{s}_j)}{2J_n} \right\} - g\mu_B \mathbf{H} \cdot \sum_{i=1}^{4} \mathbf{s}_i \right). \quad (3)$$

Here the external summation is over all the unit cells of the crystal, n enumerates magnetic shells, the sum $\{ij\}$ is over all the bonds of the shell n, the sum over i is taken over all magnetic atoms in the unit cell; $\tilde{J}_n = J_n - (D_n^2/4J_n)$, J_n is the exchange coupling interaction parameter of the nth shell, $\mathbf{D}_{n,ij}$ is the DM vector of the bond ij of the nth shell, $\mathbf{s}_i$ are classical spins of magnetic atoms, $|\mathbf{s}| = 1$, and $g\mu_B$ is the effective magnetic moment of the atom. Here we designate as a shell the set of equivalent bonds, i.e., those having the same length and connecting to each other by the symmetry transformations of the crystal space group. Thus, the nth magnetic shell unites the nth magnetic coordination spheres of all four manganese atoms in the unit cell. The terms of the order of D_n^2 are usually ignored but sometimes they can be important.[36,37]

The MnSi-type crystal has $B20$ structure ($P2_13$ space group) with four magnetic (Mn) atoms occupying crystallographically equivalent $4a$ positions within a unit cell, $\mathbf{r}_1 = (x,x,x)$, $\mathbf{r}_2 = (\frac{1}{2}-x, 1-x, \frac{1}{2}+x)$, $\mathbf{r}_3 = (1-x, \frac{1}{2}+x, \frac{1}{2}-x)$, $\mathbf{r}_4 = (\frac{1}{2}+x, \frac{1}{2}-x, 1-x)$.[38] The shortest bonds between the magnetic atoms have length $\sqrt{\frac{1}{2} - 2x + 8x^2}$. The next environment consists of two close magnetic shells with radii $\sqrt{\frac{3}{2} - 6x + 8x^2}$ and $\sqrt{\frac{1}{2} + 2x + 8x^2}$. The parameter x defines which of them is closer to the initial atom. When $x > \frac{1}{8}$ ($x \approx 0.138$ in the case of MnSi), then the shell with radius $\sqrt{\frac{3}{2} - 6x + 8x^2}$ is closer, so we will refer to it as the second one. When $x = \frac{1}{8}$, the second and third neighbors are at the same distance so that the manganese sublattice gains the space group $P4_332$,[39] connecting the second and third shells by a symmetry transformation. This could establish a linkage between the DM vectors of the shells, but the silicon sublattice (having in its turn the space group $P4_132$, when $x_{Si} = \frac{7}{8}$) breaks the symmetry and the DM vectors of the shells are different even in this case. If $x < \frac{1}{8}$, then the third neighbors become closer than the second ones.

Figure 2 shows the first three magnetic shells in MnSi. Every shell holds 12 different directed bonds between manganese atoms, which can be divided into four equilateral triangles. Besides, each triangle is perpendicular to the corresponding threefold axis passing through its center. Every manganese atom serves as a common vertex to three such triangles, thus justifying the name of the "trillium" lattice. Hence, every atom has six neighbors in each of its magnetic coordination spheres.

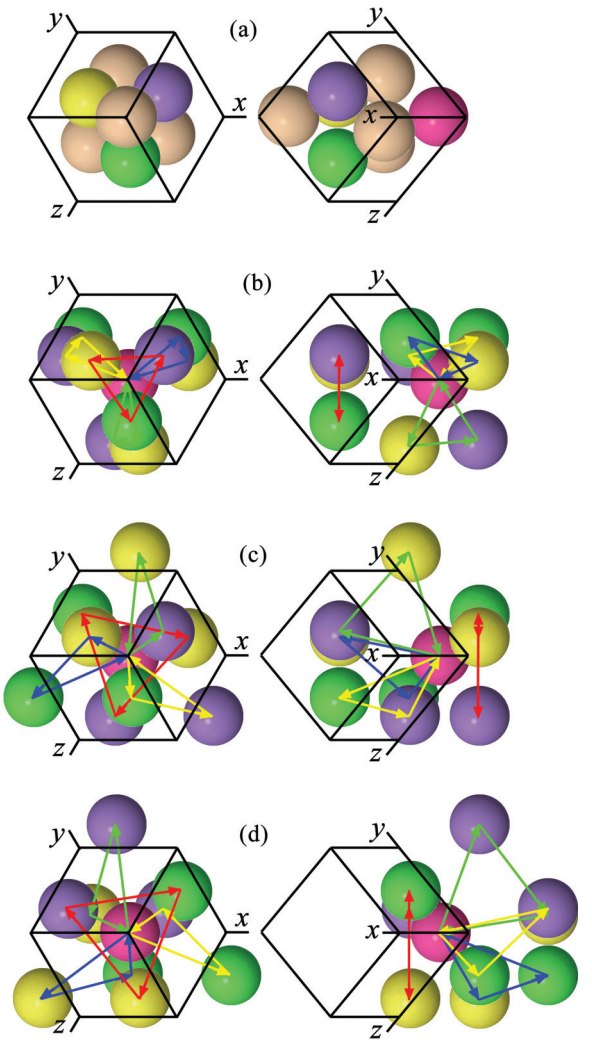

FIG. 2. (Color online) The unit cell and magnetic shells in MnSi. (a) The unit cell of the $B20$ structure (in two projections). The manganese atoms, belonging to four different magnetic sublattices, are shown as colored spheres: 1–magenta, 2–yellow, 3–violet, 4–green. Beige spheres are the silicon atoms (not shown in the next figures). (b)–(d) First, second, and third magnetic shells, correspondingly. The colored arrows designate directed bonds (12 different bonds in each shell). Shown are the neighbors of the first manganese atom (six in each shell) and atomic triangles perpendicular to the threefold axis [111].

Let (D_{1x}, D_{1y}, D_{1z}) be the coordinates of the vector $\mathbf{D}_{1,13}$ corresponding to the bond $\mathbf{b}_{1,13} = (-2x, \frac{1}{2}, \frac{1}{2} - 2x)$ directed from $\mathbf{r}_1$ to $\mathbf{r}_3 - (1,0,0)$, (D_{2x}, D_{2y}, D_{2z}) be the coordinates of the vector $\mathbf{D}_{2,13}$ corresponding to the bond $\mathbf{b}_{2,13} = (1 - 2x, \frac{1}{2}, \frac{1}{2} - 2x)$ directed from $\mathbf{r}_1$ to $\mathbf{r}_3$, and (D_{3x}, D_{3y}, D_{3z}) be the coordinates of the vector $\mathbf{D}_{3,13}$ corresponding to the bond $\mathbf{b}_{3,13} = (-2x, \frac{1}{2}, -\frac{1}{2} - 2x)$ directed from $\mathbf{r}_1$ to $\mathbf{r}_3 - (1,0,1)$.

We specify directions for all twelve bonds of a shell in a way that all directed distances $\mathbf{b}_{ij}$ between neighboring atoms connect to each other by the symmetry transformations of the point group 23, so corresponding DM vectors are connected by the same transformations. In the MnSi-type crystals there is only one type of magnetic bond directed from a central atom of type t to an atom of type $t' \neq t$ at a given shell ($n = 1,2,3$).

We can take advantage from this fact and introduce for each pair ij ($i,j = 1,2,3,4$, $i \neq j$) a local triad

$$(\boldsymbol{\tau}_i - \boldsymbol{\tau}_j) \perp (\boldsymbol{\tau}_i + \boldsymbol{\tau}_j) \perp [\boldsymbol{\tau}_i \times \boldsymbol{\tau}_j], \tag{4}$$

and then use it as a basis for vectors $\mathbf{b}_{ij}$ and $\mathbf{D}_{ij}$. Here $\boldsymbol{\tau}_i$ is a vector directed along the threefold axis passing through the position $\mathbf{r}_i$:

$$\begin{aligned} &\boldsymbol{\tau}_1 = (1,1,1), \quad \boldsymbol{\tau}_2 = (-1,-1,1), \\ &\boldsymbol{\tau}_3 = (-1,1,-1), \quad \boldsymbol{\tau}_4 = (1,-1,-1). \end{aligned} \tag{5}$$

Then the bond vector and the DM vector of an arbitrary bond in three first magnetic shells can be written as

$$\mathbf{b}_{1,ij} = (-8x+1)(\boldsymbol{\tau}_i - \boldsymbol{\tau}_j)/8 + (\boldsymbol{\tau}_i + \boldsymbol{\tau}_j)/4 + [\boldsymbol{\tau}_i \times \boldsymbol{\tau}_j]/8, \tag{6a}$$

$$\mathbf{b}_{2,ij} = (-8x+3)(\boldsymbol{\tau}_i - \boldsymbol{\tau}_j)/8 + (\boldsymbol{\tau}_i + \boldsymbol{\tau}_j)/4 - [\boldsymbol{\tau}_i \times \boldsymbol{\tau}_j]/8, \tag{6b}$$

$$\mathbf{b}_{3,ij} = (-8x-1)(\boldsymbol{\tau}_i - \boldsymbol{\tau}_j)/8 + (\boldsymbol{\tau}_i + \boldsymbol{\tau}_j)/4 - [\boldsymbol{\tau}_i \times \boldsymbol{\tau}_j]/8, \tag{6c}$$

$$\mathbf{D}_{n,ij} = \frac{D_{n+}}{4}(\boldsymbol{\tau}_i - \boldsymbol{\tau}_j) + \frac{D_{ny}}{2}(\boldsymbol{\tau}_i + \boldsymbol{\tau}_j) - \frac{D_{n-}}{4}[\boldsymbol{\tau}_i \times \boldsymbol{\tau}_j], \tag{7}$$

with $D_{n\pm} = D_{nx} \pm D_{nz}$; here $\mathbf{D}_{n,ji} \neq -\mathbf{D}_{n,ij}$ because the indices ij and ji designate two different bonds.

Notice that the energy (3) does not depend on the parameter x, so it can be chosen arbitrarily, making a convenient transition to the continuous approximation [Fig. 3(b)]. Indeed, to provide the transition the continuous unimodular vector functions will be defined, $\hat{\mathbf{s}}_1$, $\hat{\mathbf{s}}_2$, $\hat{\mathbf{s}}_3$, $\hat{\mathbf{s}}_4$, which coincide in special points with the spin values in corresponding atomic positions. If the parameter x is equal to its experimental value, e.g., $x = 0.138$ in MnSi, then we should take the functions in the real atomic positions in order to obtain the real spins. In the case of an arbitrary choice of x we should take the function values in the points shifted from the real atomic positions.

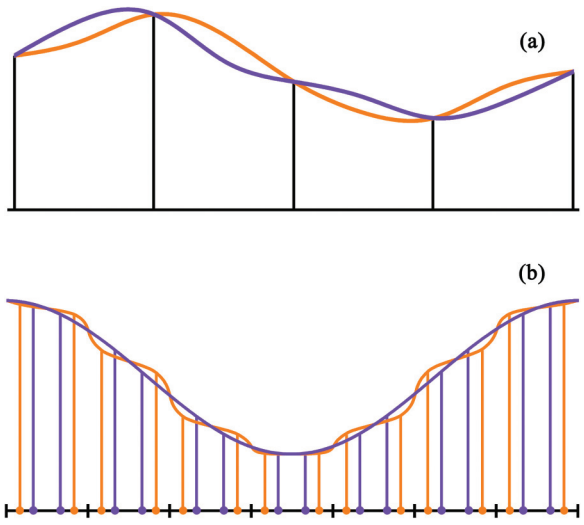

FIG. 3. (Color online) (a) The ambiguity of the transition from discrete to continuous model: two different smooth functions having equal values in a discrete set of points. (b) The gain from the arbitrary choice of the parameter x. The initial curve (orange) is plotted with the use of the function values given in the discrete set of points with the coordinates x and $\bar{x}$ within the cells of a 1D crystal. When the points are shifted to the center of the cells without a change of function values, the view of the curve changes (blue).

It is convenient to choose the parameter x from the condition

$$\sum_{n,\{ij\}} \tilde{J}_n(\boldsymbol{\tau}_i - \boldsymbol{\tau}_j) \otimes \mathbf{b}_{n,ij} = 0, \tag{8}$$

where $\otimes$ means the direct product of two vectors. Notice that this 3×3 tensor is proportional to the unit one due to the averaging over the symmetry elements of the point group 23 [see Appendix, Eq. (A2)].

Thus, for example, in the nearest-neighbors approximation the condition gives $x = \frac{1}{8}$, which is shown in Ref. 14 to be necessary in order to obtain smooth spin functions.

For $n = 1,2,3$ using Eqs. (A4) we find from Eq. (8)

$$x_{\text{exch}} = \frac{\tilde{J}_1 + 3\tilde{J}_2 - \tilde{J}_3}{8(\tilde{J}_1 + \tilde{J}_2 + \tilde{J}_3)}, \tag{9}$$

where the index "exch" means that x_{exch} is not a real coordinate, but some physical parameter expressed through the exchange interaction constants. In untwisted spin structures, the canting is determined wholly by the DM interactions. In twisted states, an extra canting arises induced by a disagreement of phases of the helices connected with different magnetic sublattices. The physical meaning of the "exchange" coordinates is that the shift of the atoms to the new positions removes the canting appearing due to the spiralling.

The bond ij of the nth shell connects the function values $\hat{\mathbf{s}}_i(\mathbf{r})$ and $\hat{\mathbf{s}}_j(\mathbf{r} + \mathbf{b}_{n,ij})$. Using continuity of the functions $\hat{\mathbf{s}}$ we can write

$$\hat{\mathbf{s}}_j(\mathbf{r} + \mathbf{b}_{n,ij}) = \mathcal{B}_{n,ij}\hat{\mathbf{s}}_j(\mathbf{r}), \tag{10}$$

where

$$\mathcal{B}_{n,ij} \equiv \exp(\mathbf{b}_{n,ij} \cdot \nabla) = 1 + (\mathbf{b}_{n,ij} \cdot \nabla) + \tfrac{1}{2}(\mathbf{b}_{n,ij} \cdot \nabla)^2 + \cdots \tag{11}$$

is the operator representing the Taylor series expansion, and pass from the summation over the unit cells to the integration over the crystal volume (in the chosen units, the lattice parameter $a = 1$ and the unit cell volume is equal to 1):

$$E = \int_V \mathcal{E}\, d\mathbf{r}, \tag{12}$$

$$\mathcal{E} = \sum_{n,\{ij\}} \{-\tilde{J}_n \hat{\mathbf{s}}_i \cdot \mathcal{B}_{n,ij}\hat{\mathbf{s}}_j + \mathbf{D}_{n,ij} \cdot [\hat{\mathbf{s}}_i \times \mathcal{B}_{n,ij}\hat{\mathbf{s}}_j] - (\mathbf{D}_{n,ij} \cdot \hat{\mathbf{s}}_i)(\mathbf{D}_{n,ij} \cdot \mathcal{B}_{n,ij}\hat{\mathbf{s}}_j)/(2J_n)\} - g\mu_B \mathbf{H} \cdot \sum_{i=1}^{4} \hat{\mathbf{s}}_i. \tag{13}$$

IV. MAGNETIC MOMENT DENSITY, CALCULUS OF VARIATIONS, AND PERTURBATION THEORY

In the phenomenological theory, the magnetic moment density $\mathbf{M}$ is used as an order parameter and considered an experimentally observed physical quantity. Nevertheless, when we try to express a smooth continuous function $\mathbf{M}$ through a discrete distribution of spins of the magnetic atoms, an ambiguity arises from the fact that we can determine the

weight function in different ways when averaging the spins on a local volume. In the present case the ambiguity has the result that the smooth functions $\hat{\mathbf{s}}_i$ having specified values in a discrete set of points can be defined in an infinite number of ways [Fig. 3(a)]. We will avoid the problem, supposing that the functions $\hat{\mathbf{s}}_i$ are defined in the most convenient way.

It would be natural to define the magnetization as

$$\mathbf{M} = 4g\mu_B\mathbf{m}, \tag{14}$$

$$\mathbf{m} = \frac{1}{4}\sum_{i=1}^{4}\hat{\mathbf{s}}_i. \tag{15}$$

In analogy with Eq. (15) we introduce the canting tensor

$$u_{\sigma\alpha} = \frac{1}{4}\sum_{i=1}^{4}\tau_{i\sigma}s_{i\alpha}, \quad \alpha,\sigma = x,y,z, \tag{16}$$

so that

$$\hat{s}_{i\alpha} = m_\alpha + \tau_{i\sigma}u_{\sigma\alpha}. \tag{17}$$

Hereinafter the summation on repeated greek indices is implied. Four conditions $|\hat{\mathbf{s}}_i| = 1, i = 1,2,3,4$, can be rewritten using the invariants

$$I_0 \equiv \frac{1}{4}\sum_{i=1}^{4}\hat{s}_i^2 = m^2 + u_{\sigma\alpha}u_{\sigma\alpha} = 1, \tag{18}$$

$$I_\sigma \equiv \frac{1}{4}\sum_{i=1}^{4}\tau_{i\sigma}\hat{s}_i^2 = 2m_\alpha u_{\sigma\alpha} + |\varepsilon_{\sigma\beta\gamma}|u_{\beta\alpha}u_{\gamma\alpha} = 0. \tag{19}$$

In order to express the energy as a functional of the magnetic moment $\mathbf{m}$, the energy should be minimized by the canting tensor components using calculus of variations. The variation of the energy is

$$\delta\tilde{E} = \int_V \delta\tilde{\mathcal{E}}\,d\mathbf{r} = \int_V \delta u_{\sigma\alpha}\Psi_{\sigma\alpha}d\mathbf{r}, \tag{20}$$

where the integrand now includes the Lagrange terms:

$$\tilde{\mathcal{E}} = \mathcal{E} + \lambda_0 I_0 + \lambda_x I_x + \lambda_y I_y + \lambda_z I_z. \tag{21}$$

Taking into account Eq. (17),

$$\begin{aligned}\Psi_{\sigma\alpha} = \sum_{n,\{ij\}}\{&-\tilde{J}_n\left[\tau_{i\sigma}\mathcal{B}_{n,ij} + \tau_{j\sigma}\mathcal{B}_{n,ij}^{-1}\right]m_\alpha\\ &-\tilde{J}_n\left[\tau_{i\sigma}\tau_{j\rho}\mathcal{B}_{n,ij} + \tau_{j\sigma}\tau_{i\rho}\mathcal{B}_{n,ij}^{-1}\right]u_{\rho\alpha}\\ &-\varepsilon_{\alpha\beta\gamma}D_{n,ij\beta}\left[\tau_{i\sigma}\mathcal{B}_{n,ij} - \tau_{j\sigma}\mathcal{B}_{n,ij}^{-1}\right]m_\gamma\\ &-\varepsilon_{\alpha\beta\gamma}D_{n,ij\beta}\left[\tau_{i\sigma}\tau_{j\rho}\mathcal{B}_{n,ij} - \tau_{j\sigma}\tau_{i\rho}\mathcal{B}_{n,ij}^{-1}\right]u_{\rho\gamma}\\ &-(1/2J_n)D_{n,ij\alpha}D_{n,ij\beta}\left[\tau_{i\sigma}\mathcal{B}_{n,ij} + \tau_{j\sigma}\mathcal{B}_{n,ij}^{-1}\right]m_\beta\\ &-(1/2J_n)D_{n,ij\alpha}D_{n,ij\beta}\left[\tau_{i\sigma}\tau_{j\rho}\mathcal{B}_{n,ij} + \tau_{j\sigma}\tau_{i\rho}\mathcal{B}_{n,ij}^{-1}\right]u_{\rho\beta}\}\\ &+2\lambda_0 u_{\sigma\alpha} + 2\lambda_\sigma m_\alpha + 2|\varepsilon_{\sigma\beta\gamma}|\lambda_\beta u_{\gamma\alpha}.\end{aligned} \tag{22}$$

Here

$$\mathcal{B}_{n,ij}^{-1} = \exp(-\mathbf{b}_{n,ij}\cdot\nabla) \tag{23}$$

and the evident equation was used, which corresponds to the integration in infinite volume,

$$\int f(\mathbf{r})\mathcal{B}g(\mathbf{r})d\mathbf{r} = \int g(\mathbf{r})\mathcal{B}^{-1}f(\mathbf{r})d\mathbf{r}. \tag{24}$$

The minimum of the energy is determined from the condition $\delta\tilde{\mathcal{E}} = 0$ with arbitrary functions $\delta u_{\sigma\alpha}$, so the problem is reduced to the system of nine equations

$$\Psi_{\sigma\alpha} = 0, \quad \sigma,\alpha = x,y,z, \tag{25}$$

with the extra conditions (18) and (19) determining the functions $\lambda_0(\mathbf{r})$, $\lambda_x(\mathbf{r})$, $\lambda_y(\mathbf{r})$, and $\lambda_z(\mathbf{r})$.

The general solution of the problem is too difficult, if possible, but we can use perturbation theory with a small parameter,

$$D/J \ll 1, \tag{26}$$

that is the ratio of typical absolute values of spin-orbit (D) and exchange (J) interactions. We assume that this parameter also describes the typical order of magnitude of spatial derivatives and the spin components responsible for the canting:

$$|\nabla| \sim |u_{\sigma\alpha}| \sim D/J. \tag{27}$$

Another quantity that can be connected with the small value of canting is $\sqrt{1-m^2}$. In a weak magnetic field, when a spiral structure still exists, $\sqrt{1-m^2} \sim D/J$. But if the field is very strong ($g\mu_B H \gg 8J$),[20] it induces a ferromagnetic alignment, and $\sqrt{1-m^2} \sim D/(g\mu_B H) \ll D/J$. In that case we can take the greater value of two parameters, D/J, as a constitutive one.

In the next section, we will use the consecutive approximations in order to find a solution of the system (25).

V. CANTING IN THE FIRST APPROXIMATION

Assuming $\lambda_\alpha^{(0)} = 0$, $\alpha = x,y,z$, the zeroth-order equations on D/J appear as

$$\sum_{n,\{ij\}}\tilde{J}_n(\tau_{i\sigma} + \tau_{j\sigma})m_\alpha = 0 \tag{28}$$

and become trivial after the summation on bonds; see Eq. (A1). The first-order equations on D/J are

$$\begin{aligned}\sum_{n,\{ij\}}\{&-\tilde{J}_n(\tau_{i\sigma} - \tau_{j\sigma})b_{n,ij\mu}\nabla_\mu m_\alpha - \tilde{J}_n(\tau_{i\sigma}\tau_{j\rho} + \tau_{j\sigma}\tau_{i\rho})u_{\rho\alpha}^{(1)}\\ &-\varepsilon_{\alpha\beta\gamma}D_{n,ij\beta}(\tau_{i\sigma} - \tau_{j\sigma})m_\gamma\} + 2\lambda_0^{(0)}u_{\sigma\alpha}^{(1)} + 2\lambda_\sigma^{(1)}m_\alpha = 0,\end{aligned} \tag{29}$$

where the upper index (p) means that the corresponding term is of the order of $(D/J)^p$. The first summand in curly brackets gives zero in accordance with Eq. (8); the two others can be calculated using Eqs. (A3f) and (A5). Then,

$$\begin{aligned}&2\left[\lambda_0^{(0)} + 4(\tilde{J}_1 + \tilde{J}_2 + \tilde{J}_3)\right]u_{\sigma\alpha}^{(1)}\\ &\quad + 8(D_{1+} + D_{2+} + D_{3+})\varepsilon_{\sigma\alpha\gamma}m_\gamma + 2\lambda_\sigma^{(1)}m_\alpha = 0.\end{aligned} \tag{30}$$

The normalization conditions are

$$u_{\sigma\alpha}^{(1)}u_{\sigma\alpha}^{(1)} = u_{\sigma\alpha}u_{\sigma\alpha} = 1 - m^2, \tag{31}$$

$$m_\alpha u_{\sigma\alpha}^{(1)} = 0, \tag{32}$$

where the first equation is of the second order on D/J.

Multiplication of Eq. (30) by m_α and summation on α with use of Eq. (32) give

$$\lambda_\sigma^{(1)} = 0, \tag{33}$$

therefore

$$u^{(1)}_{\sigma\alpha} = -\frac{4(D_{1+} + D_{2+} + D_{3+})\varepsilon_{\sigma\alpha\gamma}m_\gamma}{\lambda^{(0)}_0 + 4(\tilde{J}_1 + \tilde{J}_2 + \tilde{J}_3)}. \quad (34)$$

The substitution of Eq. (34) into Eq. (31) gives

$$\lambda^{(0)}_0 + 4(\tilde{J}_1 + \tilde{J}_2 + \tilde{J}_3) = \frac{4\sqrt{2}|D_{1+} + D_{2+} + D_{3+}|m}{\sqrt{1-m^2}}, \quad (35)$$

and, finally,

$$u^{(1)}_{\sigma\alpha} = -\operatorname{sgn}(D_{1+} + D_{2+} + D_{3+})\frac{\sqrt{1-m^2}}{\sqrt{2}m}\varepsilon_{\sigma\alpha\gamma}m_\gamma, \quad (36)$$

where the sign of the right parts of Eqs. (35) and (36) is chosen from the condition of the minimum of the canting energy.

The substitution of Eq. (36) into Eq. (17) gives

$$\hat{\mathbf{s}}_i = \mathbf{m} + \varkappa[\boldsymbol{\tau}_i \times \mathbf{m}], \quad (37)$$

with

$$\varkappa = \operatorname{sgn}(D_{1+} + D_{2+} + D_{3+})\frac{\sqrt{1-m^2}}{\sqrt{2}m}. \quad (38)$$

From Eqs. (30), (34), and (36) we conclude that the combination $D_{1+} + D_{2+} + D_{3+}$ of the DM vectors components is responsible for the canting.

VI. ENERGY DENSITY

The contributions to the energy density from the magnetic moment $\mathbf{m}$ and its derivatives are

$$\mathcal{E}^{(0)}_m = -\sum_{n,\{ij\}} \tilde{J}_n m_\alpha m_\alpha = -12(\tilde{J}_1 + \tilde{J}_2 + \tilde{J}_3)m^2, \quad (39)$$

$$\mathcal{E}^{(1)}_m = \sum_{n,\{ij\}} \{-\tilde{J}_n m_\alpha (\mathbf{b}_{n,ij}\cdot\nabla)m_\alpha + \varepsilon_{\alpha\beta\gamma}D_{n,ij\alpha}m_\beta m_\gamma\} = 0, \quad (40)$$

$$\mathcal{E}^{(2)}_m = \sum_{n,\{ij\}} \left\{-\frac{1}{2}\tilde{J}_n m_\alpha (\mathbf{b}_{n,ij}\cdot\nabla)^2 m_\alpha + \varepsilon_{\alpha\beta\gamma}D_{n,ij\alpha}m_\beta(\mathbf{b}_{n,ij}\cdot\nabla)m_\gamma - (2J_n)^{-1}D_{n,ij\alpha}D_{n,ij\beta}m_\alpha m_\beta\right\}. \quad (41)$$

Using Eqs. (A7), (A8), and (A6) with $x = x_{\text{exch}}$ we obtain

$$\mathcal{E}^{(2)}_m = -\mathcal{J}\mathbf{m}\cdot\Delta\mathbf{m} + \mathcal{D}\mathbf{m}\cdot[\nabla\times\mathbf{m}] - \left(\frac{2D_1^2}{J_1} + \frac{2D_2^2}{J_2} + \frac{2D_3^2}{J_3}\right)m^2, \quad (42)$$

with

$$\mathcal{J} = \frac{3\tilde{J}_1^2 + 3\tilde{J}_2^2 + 3\tilde{J}_3^2 + 10\tilde{J}_1\tilde{J}_2 + 10\tilde{J}_1\tilde{J}_3 + 22\tilde{J}_2\tilde{J}_3}{4(\tilde{J}_1 + \tilde{J}_2 + \tilde{J}_3)}, \quad (43)$$

$$\begin{aligned}\mathcal{D} &= -4(\mathbf{D}_{1,13}\cdot\mathbf{b}_{1,13} + \mathbf{D}_{2,13}\cdot\mathbf{b}_{2,13} + \mathbf{D}_{3,13}\cdot\mathbf{b}_{3,13})\\ &= 8x_{\text{exch}}(D_{1+} + D_{2+} + D_{3+}) - (D_{1+} - D_{1-} + 2D_{1y})\\ &\quad - (3D_{2+} + D_{2-} + 2D_{2y}) - (-D_{3+} + D_{3-} + 2D_{3y}).\end{aligned} \quad (44)$$

Notice that though the components D_x, D_y, D_z are included in Eq. (44) in a nonsymmetrical way, it does not break the cubic symmetry of the crystal. Indeed, D_{nx}, D_{ny}, D_{nz} are nothing but the components of an arbitrarily chosen DM vector from the nth magnetic shell, and the appearance of Eq. (44) depends on which of the twelve DM vectors of the shell we consider as the first one.

The first term in Eq. (42) can be rewritten as

$$\mathcal{J}\frac{\partial m_\alpha}{\partial r_\beta}\frac{\partial m_\alpha}{\partial r_\beta} - \frac{1}{2}\mathcal{J}\nabla\cdot(\nabla m^2), \quad (45)$$

where the second term gives a contribution to the surface energy only:

$$-\frac{1}{2}\mathcal{J}\int_V d\mathbf{r}\nabla\cdot(\nabla m^2) = -\frac{1}{2}\mathcal{J}\oint_S d\mathbf{f}\cdot\nabla m^2. \quad (46)$$

Far from the transition between paramagnetic and ferromagnetic states, the absolute value m of the magnetic moment changes slowly, and this contribution to the energy can be neglected. However, near the phase transition, m can undergo considerable changes, and in crystals with a significant surface (nanocrystals, thin films) the term (46) could play an important role. In particular, it could be important for the stabilization of the A phase observed in thin films of $Fe_{0.5}Co_{0.5}Si$ and FeGe.[40,41]

The contributions from the canting to the energy density are

$$\mathcal{E}^{(1)}_u = -\sum_{n,\{ij\}} \tilde{J}_n(\tau_{i\sigma} + \tau_{j\sigma})u^{(1)}_{\sigma\alpha}m_\alpha = 0, \quad (47)$$

$$\begin{aligned}\mathcal{E}^{(2)}_u &= \sum_{n,\{ij\}}\{-\tilde{J}_n(\tau_{i\sigma} - \tau_{j\sigma})u^{(1)}_{\sigma\alpha}(\mathbf{b}_{n,ij}\cdot\nabla)m_\alpha\\ &\quad - \tilde{J}_n(\tau_{i\sigma} + \tau_{j\sigma})u^{(1)}_{\sigma\alpha}m_\alpha - \tilde{J}_n\tau_{i\sigma}\tau_{j\rho}u^{(1)}_{\sigma\alpha}u^{(1)}_{\rho\alpha}\\ &\quad + \varepsilon_{\alpha\beta\gamma}D_{n,ij\alpha}(\tau_{i\sigma} - \tau_{j\sigma})u^{(1)}_{\sigma\beta}m_\gamma\}\\ &= 4(\tilde{J}_1 + \tilde{J}_2 + \tilde{J}_3)u^{(1)}_{\sigma\alpha}u^{(1)}_{\sigma\alpha}\\ &\quad + 8(D_{1+} + D_{2+} + D_{3+})\varepsilon_{\sigma\beta\gamma}u^{(1)}_{\sigma\beta}m_\gamma\\ &= 4(\tilde{J}_1 + \tilde{J}_2 + \tilde{J}_3)(1-m^2)\\ &\quad - 8\sqrt{2}|D_{1+} + D_{2+} + D_{3+}|m\sqrt{1-m^2}.\end{aligned} \quad (48)$$

Thus, we can finally rewrite the bulk energy density as a function of the magnetic moment $\mathbf{m}$ accurate within the second-order terms on D/J:

$$\begin{aligned}\mathcal{E} &= \mathcal{J}\frac{\partial m_\alpha}{\partial r_\beta}\frac{\partial m_\alpha}{\partial r_\beta} + \mathcal{D}\mathbf{m}\cdot[\nabla\times\mathbf{m}]\\ &\quad + (\tilde{J}_1 + \tilde{J}_2 + \tilde{J}_3)(4 - 16m^2)\\ &\quad - 8\sqrt{2}|D_{1+} + D_{2+} + D_{3+}|m\sqrt{1-m^2}\\ &\quad - \left(\frac{2D_1^2}{J_1} + \frac{2D_2^2}{J_2} + \frac{2D_3^2}{J_3}\right)m^2 - 4g\mu_B\mathbf{H}\cdot\mathbf{m}.\end{aligned} \quad (49)$$

The first two terms with derivatives are nothing but the deformation energy of the conventional phenomenological theory of the chiral magnetics. However, here the values $\mathcal{J}$ and $\mathcal{D}$ are expressed through the parameters of the microscopic theory accordingly to Eqs. (43) and (44). The following term,

on condition that $m \approx 1$, gives $-12(\tilde{J}_1 + \tilde{J}_2 + \tilde{J}_3)$; that is, the energy of 36 ferromagnetic bonds in first three shells in the unit cell. Then, the term with $\sqrt{1-m^2}$ is the contribution of the canting. It is always negative, which means that the canting is an important and unavoidable peculiarity of the magnetic structures of MnSi-type crystals. When minimizing the energy on m, this term gives a contribution to the derivative proportional to $1/\sqrt{1-m^2}$, which becomes dominant, when $m \to 1$–0, impeding m from exceeding 1.

VII. EXTRA TWIST INDUCED BY CANTING

Now we return to Eq. (44), which defines the DM parameter $\mathcal{D}$ of the phenomenological theory. As it was mentioned above, from the physical point of view, the DM vectors are almost perpendicular to the corresponding bonds and, consequently, the expected value of $\mathcal{D}$ is small. In Ref. 20 some speculative estimation has been performed with use of the well known Keffer rule[42] based on the Moriya theory,[18] which gives us following expression for the DM vector:

$$\mathbf{D}_{12} = D[\mathbf{r}_{1i} \times \mathbf{r}_{2i}], \tag{50}$$

where D is unknown coefficient, and the vectors $\mathbf{r}_{1i}$ and $\mathbf{r}_{2i}$ are directed from the positions of first and second magnetic (Mn) atoms to that of an intermediate nonmagnetic (Si) atom realizing the spin-orbit interaction. It is evident that $\mathbf{D}_{12} \perp \mathbf{r}_{12} = \mathbf{r}_{2i} - \mathbf{r}_{1i}$.

For the Keffer rule one needs the constants D and coordinates of different intermediate atoms. Surprisingly, a considerable result can be achieved with a more general rule, namely that the DM vectors are perpendicular to the bonds. The condition can be written as

$$\mathbf{D} \cdot \mathbf{b}(x = x_{\text{real}}) = 0, \tag{51}$$

and, comparing with Eq. (44), we easily find in this case that

$$\mathcal{D} = 8(D_{1+} + D_{2+} + D_{3+})(x_{\text{exch}} - x_{\text{real}}), \tag{52}$$

which gives us a new definition of the exchange coordinate as the manganese atom position inhibiting spiralling when combining with the Keffer rule. The combination $D_{1+} + D_{2+} + D_{3+}$ is responsible for the canting in accordance with Sec. V, and x_{exch} is a combination of the exchange interaction constants. Equation (52) can be interpreted as evidence of the canting's direct participation in the magnetic structure spiralling. Besides, the sign of $\mathcal{D}$ and consequently the magnetic chirality are determined both by the sign of the canting component $D_{1+} + D_{2+} + D_{3+}$ of the DM vectors and that of the difference $x_{\text{exch}} - x_{\text{real}}$, depending on the exchange constants $\tilde{J}_1$, $\tilde{J}_2$, and $\tilde{J}_3$.

Therefore, the canting, initially considered as a supplementary microscopic peculiarity of the chiral magnetics,[14,20] can be in fact an essential cause of the twisting power. Let us demonstrate by a simple, albeit not very realistic, example how the canting between different magnetic sublattices can result in an essential twist gain. We consider a periodical 1D chain of spins with a local interaction between them, composed of unit cells containing two spins, say A and B (Fig. 4). All the spins can rotate in a plane, and the energy of the chain is a

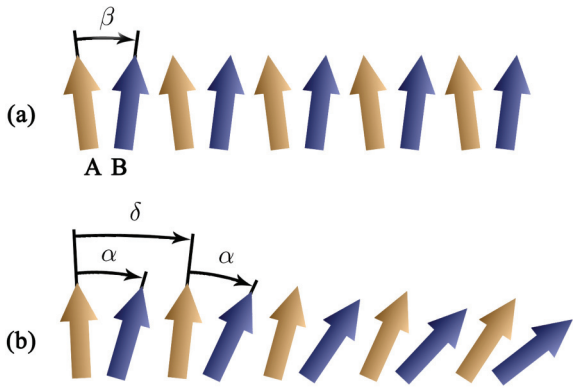

FIG. 4. (Color online) Periodical 1D chain of magnetic atoms with two spins within a unit cell. The spins can rotate in a plane, and their directions are fully determined by the only variable φ. The spin interaction is described by the classic Hamiltonian (53). (a) When $J = 0$, the chirality is hidden; the lattice is divided onto two sublattices with the ferromagnetic ordering of spins and the canting angle β between them. (b) When an additional ferromagnetic interaction with the atoms of the alternate kind is included ($J > 0$), the chirality becomes apparent in the magnetic helix with the angle δ between neighboring unit cells; besides, the angle α between the atoms A and B within a cell remains the same over the chain.

function of differences of the angles:

$$E = \sum_n \{C_R(\varphi_n^A - \varphi_n^B + \beta)^2 + C_L(\varphi_n^A - \varphi_{n-1}^B + \beta)^2 + J(\varphi_n^A - \varphi_n^B)^2 + J(\varphi_n^A - \varphi_{n-1}^B)^2\}. \tag{53}$$

Here φ_n^A and φ_n^B are orientation angles of the spins A and B of the nth cell, with respect to an arbirary direction; C_R and C_L are positive constants. The condition $C_R \neq C_L$ determines the chirality of the structure.

When $J = 0$, Eq. (53) describes a periodical magnetic structure with the angle β of canting between the spin sublattices A and B [Fig. 4(a)]. We suppose that this structure is a result of the competition of two ordering interactions between neighboring spins: a ferromagnetic one and a twisting chiral one; besides, there is a reason, which is not considered here, for elimination of the twist in this state.

The question arises: What happens with the structure after introducing of an additional ferromagnetic ($J > 0$) interaction with the nearest neighbors from the complementary sublattice? The minimization of Eq. (53) gives the solution in the helix form

$$\varphi_n^A = n\delta, \quad \varphi_n^B = n\delta + \alpha, \tag{54}$$

where

$$\alpha = \frac{C_R \beta}{C_R + J} \tag{55}$$

is a tilt angle between spins in the unit cell, and

$$\delta = \frac{J(C_R - C_L)\beta}{(C_R + J)(C_L + J)} \tag{56}$$

is the twist angle per one period of the chain [Fig. 4(b)].

At the first sight it seems to be paradoxical that introducing an additional aligning interaction induces a twist, but a simple analysis of the problem shows that there is no contradiction here. When $|J| \to \infty$, the angles α and δ go to zero as expected. In order to understand the system behavior for finite values of J, consider the numerator of Eq. (56). The factor $(C_L - C_R)$ reflects the degree of the internal chirality of the structure. The product $J\beta$ reminds us of a lever torque, with β playing the role of the lever arm and J being analogous to the rotating force. We can imagine that the "aligning force" J, being applied to the initially tilted by the angle β sublattices, results in structure distortions, which in their turn induce the twist due to the potential chirality of the structure $(C_R \neq C_L)$. Notice that the change of the sign of the constant J, corresponding to the transition from ferromagnetic $(J > 0)$ to antiferromagnetic $(J < 0)$ coupling, increases the degree of the twist (reduces the helix pitch) and changes its handedness.

We expect that a similar effect takes place in chiral magnetic MnSi. Indeed, there is an evident similarity of Eqs. (52) and (56). In this case the role of a lever is played by the canting induced by the DM interactions, whereas the "force" is the ferro- or antiferromagnetic aligning interaction with neighboring atoms.

VIII. ESTIMATION OF THE EXCHANGE PARAMETERS AND THE RKKY THEORY

In analogy with the Dzyaloshinskii-Moriya interaction, the exchange one is described differently in microscopical and phenomenological approaches. Although it is evident that the exchange constants of both theories should be connected to each other, the connection is found in the nearest-neighbors approximation[14] to be not so trivial as we could expect. Indeed, the expression (43) for $\mathcal{J}$ in the approximation of three magnetic shells is significantly different from the simple proportionality in the former case. However, the situation seems to be even more intricate, because $\mathcal{J}$ is not sufficient to induce the ferromagnetic alignment, and another exchange parameter is also needed, namely

$$J_\Sigma = \sum_j \tilde{J}_j, \tag{57}$$

where the summation is taken over all the neighbors contributing to the exchange interaction. Then the condition of the validity of our approximation can be written as two inequalities,

$$J_\Sigma > 0, \tag{58}$$

$$\mathcal{J} > 0, \tag{59}$$

both equally important. Here J_Σ is nothing but the energy of an individual spin interaction with its magnetic surroundings in the untwisted (ferromagnetic) state, taken with an opposite sign, and Eq. (58) guarantees stability of the state relative to the change of the spin sign. Equation (59) in its turn guarantees stability relative to the spin small rotations, providing the smallness of the magnetic moment gradients. Therefore, only combined use of the conditions leads to a ferromagnetic ordering with a weak spiralling.

Neglecting the contribution of the DM interaction to symmetrical exchange (i.e., using J_n instead of $\tilde{J}_n$), we can estimate J_Σ and $\mathcal{J}$ in the frame of the RKKY theory,[43–46] which is applicable to the itinerant magnetics. Indeed, in this model J_n is a simple function of the distance between interacting atoms,

$$J_n \equiv J(b_n) \sim -F(2k_F a b_n), \tag{60}$$

$$F(x) = \frac{x\cos x - \sin x}{x^4}. \tag{61}$$

Here k_F is the Fermi wave number, and b_n is the dimensionless length of the bonds of the nth magnetic shell.

It follows from Eqs. (60) and (61) that atoms situated at approximately the same distances, e.g., b_2 and b_3, make similar contributions to the exchange energy. Therefore, together with the second and third shells it is necessary to take into account the fourth shell corresponding to the atoms separated by lattice periods. Because the atoms of the fourth shell belong to the same magnetic sublattice, they do not affect the canting between different sublattices, i.e., they leave $u_{\sigma\alpha}$ and x_{exch} unchanged and give simple additive contributions to J_Σ and $\mathcal{J}$.

All the magnetic spheres of an atom have six atoms, so

$$J_\Sigma = 6(J_1 + J_2 + J_3 + J_4). \tag{62}$$

In order to calculate the additive from the fourth shell to $\mathcal{J}$, we can write, for example, the interaction energy of two spins separated by the period (1,0,0) of the lattice,

$$-J_4\mathbf{s}(\mathbf{r})\cdot\mathbf{s}(\mathbf{r}+(1,0,0)) \approx -J_4\left(1 + \mathbf{s}\cdot\frac{\partial\mathbf{s}}{\partial x} + \frac{1}{2}\mathbf{s}\cdot\frac{\partial^2\mathbf{s}}{\partial x^2}\right). \tag{63}$$

If we take the sum over six bonds, multiply it by the number of magnetic atoms in the unit cell and take into account that all the bonds in that sum are taken twice, then the correction to the energy density can be written as

$$\Delta\mathcal{E} = -12J_4 - 2J_4\mathbf{m}\cdot\Delta\mathbf{m}. \tag{64}$$

It is obvious from the comparison with Eq. (42) that the additive to $\mathcal{J}$ from the fourth magnetic shell is $2J_4$.

The parameters $F_n \equiv F(2k_F a b_n)$ are oscillating functions of the argument $k_F a$, which are easy to calculate using real distances between magnetic atoms. In MnSi for $x = 0.138$ we find $b_1 = 0.613$, $b_2 = 0.908$, $b_3 = 0.964$, and $b_4 = 1$. Figure 5(a) shows the functions F_1–F_4 plotted in the area $10 < k_F a < 20$, where the value $k_F a = 16.4$ for MnSi is situated ($k_F = 3.6$ Å^{-1},[47] $a = 4.56$ Å). The graphs show that Eqs. (58) and (59) can be satisfied together in the areas of negative values of F_1. Figure 5(b) represents dependences of J_Σ and $\mathcal{J}$ on $k_F a$, calculated for the same area. Both J_Σ and $\mathcal{J}$ are oscillating alternating-sign functions; the jumps of $\mathcal{J}$ correspond to the zeros of $J_1 + J_2 + J_3$. The nearest to the value $k_F a = 16.4$ "plateau" with positive J_Σ and $\mathcal{J}$ is in the area $17.1 < k_F a < 18.9$.

Notice that the behavior of $\mathcal{J}$ at some $k_F a$ could seem paradoxical. For example, the divergence of $\mathcal{J} \to +\infty$ would mean a strong suppression of long-wavelength fluctuations. However, the paradox can be resolved by taking into account the behavior of J_Σ. Indeed, if $J_1 + J_2 + J_3 = 0$, then $J_\Sigma \sim J_4$,

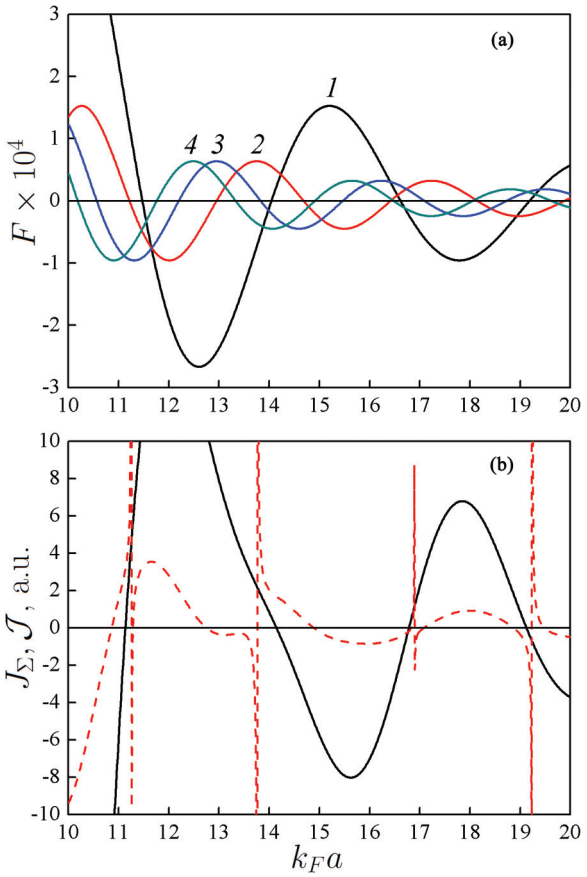

FIG. 5. (Color online) (a) The $F_n \equiv F(2k_F a b_n)$ dependences on the Fermi wave number for four magnetic shells. The distances b_1–b_4 are chosen as for MnSi. The minima of F_1 give the areas with $J_\Sigma, \mathcal{J} > 0$. (b) The J_Σ (solid line) and $\mathcal{J}$ (dashed line) dependences on the Fermi wave number. The plots show strong oscillations. The jumps of $\mathcal{J}$ correspond to the zeros of $J_1 + J_2 + J_3$. The areas with $J_\Sigma, \mathcal{J} > 0$ determine weakly twisted ferromagnetic states. The plateau closest to the known value for MnSi, $k_F a = 16.4$, is in the area $17.1 < k_F a < 18.9$.

where J_4 is nothing but the coupling constant of the spins belonging to the same sublattice. This means that, when $\mathcal{J} \to +\infty$, the connection between sublattices gets broken. Thus, when the spins of three sublattices are aligned in the same direction, the spins of the fourth one can have an arbitrary direction, even if the condition $J_4 > 0$ guarantees the ferromagnetic order within the sublattice. The foregoing means that in addition to Eqs. (58) and (59), we should introduce another inequality,

$$J'_\Sigma = \sum_j{}' \tilde{J}_j > 0, \tag{65}$$

determining the ferromagnetic connection of the four magnetic sublattices. Here the sum is taken over the bonds connecting atoms belonging to different sublattices. In the approximation of four magnetic shells, $J'_\Sigma = 6(J_1 + J_2 + J_3) = J_\Sigma - 6J_4$, therefore the zeros of J'_Σ coincide with the jumps of $\mathcal{J}$.

The RKKY model allows us as well to estimate the exchange coordinate x_{exch}. Because, according to Eq. (52), the degree of the twist is determined by the difference $x_{\text{exch}} - x_{\text{real}}$, it is useful to have an idea about how much this difference could

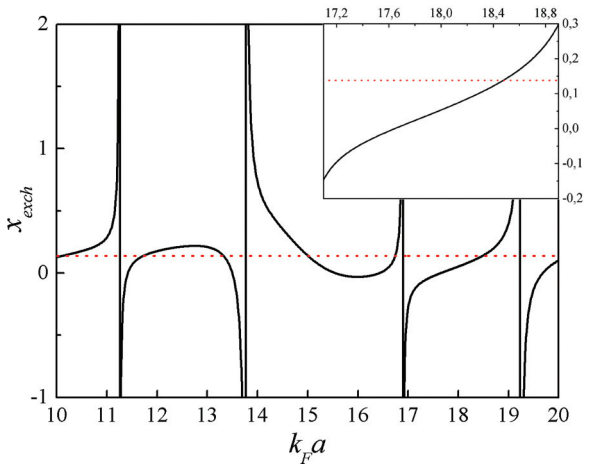

FIG. 6. (Color online) Exchange coordinate x_{exch} calculated in the RKKY model. The jumps of the function correspond to the zeros of $J_1 + J_2 + J_3$. The dotted line identifies the real value $x_{\text{real}} = 0.138$ for MnSi. The inset shows the x_{exch} dependence in the area corresponding to positive J_Σ and $\mathcal{J}$, $17.1 < k_F a < 18.9$, where $-0.28 < x_{\text{exch}} - x_{\text{real}} < 0.16$. The chirality of the magnetic structure change its sign when $x_{\text{exch}} = x_{\text{real}}$.

be. In the nearest-neighbors approximation $x_{\text{exch}} = \frac{1}{8}$, which is close to the real value $x_{\text{real}} = 0.138$ for MnSi. However, when taking into account the contributions from the second and third shells, x_{exch} can have arbitrary large positive and negative values near the zeros of $J_1 + J_2 + J_3$ (Fig. 6). Close to the minima of F_1, J_2 and J_3 are small in comparison with J_1 and, therefore, $x_{\text{exch}} \approx \frac{1}{8}$; see the inset in Fig. 6. Notice that the zeros of $J_1 + J_2 + J_3$ do not result in a divergence of the wave number $k = \mathcal{D}/2\mathcal{J}$, because $\mathcal{J}$ in the denominator and x_{exch} in the numerator increase simultaneously.

As seen in from Fig. 6 and its inset, the difference $x_{\text{exch}} - x_{\text{real}}$ can change its sign depending on k_F. This gives a possibility to control the magnetic structure chirality by varying the concentration of different elements in the crystal.

Equations (58) and (59) are evident preconditions of the experimentally observed ferromagnetic order in MnSi. Nevertheless, we can not preclude that one of the constants J_Σ, $\mathcal{J}$, or both these parameters, can have negative values. For example, the condition $J_\Sigma < 0$ does not surely result in an antiferromagnetic order. The strong frustrations intrinsic in the system, e.g., the triangles of bonds, and nonisotropic DM interactions can induce a small magnetic moment and lead to a ferri- or a weak ferromagnetic order. This could explain the weak magnetic moment observed in MnSi ($g \approx 0.4$). When $\mathcal{J} < 0$, the contributions to the energy density with higher spatial derivatives should be taken into account, which can stabilize the helix pitch.

IX. CANTING AND MAGNETIC DIFFRACTION

In Sec. V, we obtain Eq. (37), which says that in the first approximation the canting can be described as spin rotations by the same small angle around corresponding threefold axes. A similar expression for the ferromagnetic state caused by a strong magnetic field was found in Ref. 20, where an approach was suggested to measure the canting using neutron or x-ray

magnetic diffraction. In Ref. 20, the angle of spin tilt was proportional to $\delta = D_{1+}/4J_1$. In order to obtain that result we can find the coefficient $\varkappa \sim \sqrt{1-m^2}/\sqrt{2}m$ for untwisted state. The minimization of Eq. (49) on magnetic moment modulus m, assuming that $\mathbf{H} \parallel \mathbf{m} = \text{const}$, gives

$$\varkappa = \frac{D_{1+} + D_{2+} + D_{3+}}{4(J_1 + J_2 + J_3 + g\mu_B H/8)}. \tag{66}$$

Notice that $\varkappa = \delta$, when $D_2 = D_3 = J_2 = J_3 = H = 0$. The corresponding expressions for the structure factors of purely magnetic reflections $00\ell(\ell = 2n+1)$ can be easily found from Ref. 20.

Notice that there is another contribution to the reflections, induced by the anisotropy of magnetic susceptibility tensor.[48,49] The contributions can be distinguished because (i) the tilts have different directions, and (ii) the canting effect does not depend on the magnetic field modulus, whereas the tilts induced by the susceptibility tensor anisotropy are proportional to H.

The fact that both the twist and canting are determined by the same DM vectors components gives an additional possibility of numerical verification of the theory. Indeed, excluding $D_{1+} + D_{2+} + D_{3+}$ from Eqs. (66) and (52), we can connect the canting angle in the unwound state and the wave number $k = \mathcal{D}/2\mathcal{J}$ of the magnetic helices:

$$\varkappa = \frac{\mathcal{J}}{16(J_1 + J_2 + J_3 + g\mu_B H/8)(x_{\text{exch}} - x_{\text{real}})} k. \tag{67}$$

Excepting observable physical values, Eq. (67) contains only exchange interaction constants, which are easier to calculate using *ab initio* methods than the DM vectors.

X. SUMMARY AND DISCUSSION

An essential difference of the microscopic description of the magnetic properties of MnSi-type crystals from the phenomenological one is the usage of the pseudovector **D** instead of pseudoscalar $\mathcal{D}$ when describing the Dzyaloshinskii-Moriya interaction. The presence of the extra parameters (pseudovector components) results in the existence of a local canting, a feature not studied yet in magnetic twisted structures. An important problem solved in the present work is how to distinguish the components of **D** responsible for the twist and the canting. Hopkinson and Kee in Ref. 19 showed numerically (in the nearest neighbors approximation) that the components of the **D** vectors lying along the bonds were responsible for the twist, whereas the **D** components directed perpendicular to the bonds and lying in the planes of bond triangles in the trillium lattice were responsible for the canting. In Ref. 14 we specified the result and showed that real components of **D** inducing the twist and the canting lay along crystallographic directions closed to those found in Ref. 19. Nevertheless, the problem remained that, in accordance with the quantum mechanical description, the DM vectors should be perpendicular or almost perpendicular to the bonds. In other words, the **D** components responsible for the twist accordingly to Refs. 14 and 19 could be diminutive. In order to solve the problem we take into account the contribution of non-nearest neighbors in the magnetic interaction. Surprisingly, it appears that in the case, when all the DM vectors are perpendicular to the bonds, the spiralling is determined by the same **D** components as the canting. It leads to the conclusion that the canting, initially being considered as an additional microscopic effect in relation to the global twist, can in fact serve as a cause of the abnormal twist experimentally found in MnSi-type crystals, particularly in MnGe. It is also important that the contribution of non-nearest magnetic neighbors should be taken into account.

In the simplest phenomenological theory describing twisted magnetic structures, it is supposed that $|\mathbf{M}| = \text{const}$, which is roughly true at low temperatures, far below the phase transition from the paramagnetic state. However, this condition makes energetically unfavorable such structures as the Skyrmions and their lattices, associated with the A phase observed close by the transition point. In order to overcome this problem as well as to describe the critical phenomena, two additional terms, M^2 and M^4, limiting the value of magnetic moment are included in the free energy.[16] The presence of the terms decreases M in the regions with a large density of the magnetic energy, thereby decreasing the energy of the whole structure. Thus, in Ref. 50 the terms M^2 and M^4 are used in order to calculate the energy of Skyrmions. It is found that M decreases considerably nearby the core of the Skyrmion, where the magnetic moment **M** has a direction opposite to the external magnetic field, and has a maximum at some distance from the core, where the energy gain from the double twist is maximal. However, in the latter case the magnetic moment exceeds its saturation value M_0, which is not acceptable for physical reasons. In the present work we show that there should be a contribution from the canting $\sim m\sqrt{1-m^2}$ to the energy density, which can play the same role as M^2 and M^4, but does not allow the magnetic moment modulus to exceed the saturation threshold. Besides the canting, the thermal fluctuations of spins also contribute to the reduction of the magnetic moment M. Near the transition point the amplitude of the fluctuations can be comparable with the canting. Moreover, the lower the effective local field $\mathbf{h}_{\text{eff},i} = -\partial E/\partial \mathbf{s}_i$ is, acting on the individual spin $\mathbf{s}_i$, the greater the fluctuations and cantings. Therefore, the reinforcements of both the thermal fluctuations and the canting have the same cause, so they should give a similar effect.

If the canting were to be observed in MnSi, direct confirmation of a non-nearest-neighbors effect could be possible using Eq. (67), connecting the propagation number of the magnetic helices with the magnitude of the residual canting in the unwound state in a strong magnetic field. The equation involves only the exchange constants J_n and does not depend on the DM vectors. The possibility of an experimental proof of the theory should stimulate *ab intio* calculations of the interaction constants. Some semiquantitative estimations are made in the present work with use of the RKKY model. However, problems still remain. For example, the RKKY parameter $k_F a = 16.4$ for MnSi corresponds to the area, where $J_\Sigma < 0$ and $\mathcal{J} < 0$. More realistic calculations would give a tip about the direction of a further search.

It has been found in Ref. 51 that the propagation number k of the magnetic helix in the alloy $Fe_{1-x}Co_xSi$ is strongly

dependent on the concentration x of the cobalt atoms. Thus, when x changes from 0.05 to 0.15, the helix period decreases abruptly by several times. It can be explained, in particular, by the strong dependence of the Fermi wave number k_F on the cobalt impurity concentration, which also effects the exchange parameters J_Σ, $\mathcal{J}$, and x_{exch}. This phenomenon could be also responsible for the recently observed[52,53] change of the sign of the magnetic helicity in $Mn_{1-x}Fe_xGe$ alloys. Indeed, from Eq. (52) the correlation follows between the crystalline chirality Γ_c and the magnetic helicity γ_m. Thus, for the left-handed structure ($\Gamma_c = -1$), described in Sec. III, the magnetic helicity

$$\gamma_m = \operatorname{sgn} \mathcal{D} = \operatorname{sgn}(D_{1+} + D_{2+} + D_{3+}) \operatorname{sgn}(x_{\text{exch}} - x) \tag{68}$$

($\mathcal{D} > 0$ corresponds to the right magnetic helix). The first multiplier in the right part of Eq. (68) is the sign of some combination of the DM vectors components, whereas the second one depends on the isotropic exchange parameters. Equation (68) shows that the helicity γ_m can change even if the microscopic DM interaction, defined by the vectors $\mathbf{D}$, remains constant. In this case the sign change is due to the interplay between the exchange parameters J_1, J_2, and J_3 of three magnetic shells. This is drastically different from the usually supposed change of the sign of the DM interaction. Thus, a potential possibility arises to control the sign of the magnetic chirality by varying the concentration of the different components and therefore affecting the Fermi wave number k_F. Notice that the possibility of such an effect becomes evident only when the interactions with non-nearest neighbors are taken into account.

Another interesting fact, not yet explained within the framework of microscopic theories, is the helix ordering along some special directions, e.g., $\langle 111 \rangle$ or $\langle 100 \rangle$. Usually this ordering is associated with a weak anisotropic exchange,[16] but in fact the ordinary DM interaction also can result in the appearance of cubic anisotropic terms in the energy of spiral orientation in the lattice with a cubic space group. These contributions of order $(D/J)^4$ will determine the critical magnetic field H_{c1}, at which the helix comes off of its preferable zero-field direction. This is in good agreement with the observed ratio of the first and second critical fields $H_{c1} \ll H_{c2}$, because it follows from our estimations that $H_{c1}/H_{c2} \sim (D/J)^2$. Indeed, as an example, the period of the magnetic helix in MnSi yields about 40 unit cell parameters, which gives the value $2\pi/40$ for the propagation number modulus $|k|$. On the other hand, it follows from the phenomenological description that $k = \mathcal{D}/(2\mathcal{J})$, or $D/J \sim \pi/10 \approx 0.3$. This gives us the estimation $H_{c1}/H_{c2} \sim 0.1$, which is in good agreement with the experimental data. In our previous work[14] we proposed a coarse-grain approximation, which allowed us to calculate only the contributions to the energy proportional to $(D/J)^2$. In the present work a new approach has been developed permitting more precise calculations of the energy. In particular, the terms of the order of $(D/J)^4$ would give us a contribution of the Dzyaloshinskii-Moriya interaction to the energy of the cubic anisotropy responsible for (i) the ordering of the spiral axes along selected crystallographic directions, e.g., $\langle 111 \rangle$ in MnSi, in the absence of external magnetic field; and (ii) the orientation of the triangle Skyrmion lattice in the A phase observed in these crystals.[7–9]

ACKNOWLEDGMENTS

We are grateful to M. V. Gorkunov, S. V. Demishev, S. V. Maleyev, S. V. Grigoriev, V. A. Dyadkin, and S. S. Doudoukine for useful discussions and encouragement. This work was supported by two projects of the Presidium of the Russian Academy of Sciences: "Matter at high energy densities; Substance under high static compression" and "Diffraction of synchrotron radiation in multiferroics and chiral magnetics."

APPENDIX

The vectors $\boldsymbol{\tau}_i$, $\boldsymbol{\tau}_j$, $(\boldsymbol{\tau}_i - \boldsymbol{\tau}_j)$, $(\boldsymbol{\tau}_i + \boldsymbol{\tau}_j)$, $[\boldsymbol{\tau}_i \times \boldsymbol{\tau}_j]$, $\mathbf{b}_{n,ij}$, $\mathbf{D}_{n,ij}$ $(n = 1,2,3)$ change with use of the same symmetry transformations of the point group 23, when the index ij passes trough 12 possible values $\{12,13,14,21,23,24,31,32,34,41,42,43\}$. Therefore we can use the formulas

$$\sum_{\{ij\}} \mathbf{a}_{ij} = 0, \tag{A1}$$

$$\sum_{\{ij\}} a_{ij\alpha} b_{ij\beta} = 4(\mathbf{a}_{12} \cdot \mathbf{b}_{12}) \delta_{\alpha\beta}, \tag{A2}$$

where $\mathbf{a}_{ij}$ and $\mathbf{b}_{ij}$ are the vectors from the above-listed set. Thereby the following summations can be easily made:

$$\sum_{\{ij\}} (\boldsymbol{\tau}_i - \boldsymbol{\tau}_j)_\alpha (\boldsymbol{\tau}_i + \boldsymbol{\tau}_j)_\beta = 0, \tag{A3a}$$

$$\sum_{\{ij\}} (\boldsymbol{\tau}_i \pm \boldsymbol{\tau}_j)_\alpha [\boldsymbol{\tau}_i \times \boldsymbol{\tau}_j]_\beta = 0, \tag{A3b}$$

$$\sum_{\{ij\}} (\boldsymbol{\tau}_i - \boldsymbol{\tau}_j)_\alpha (\boldsymbol{\tau}_i - \boldsymbol{\tau}_j)_\beta = 32 \delta_{\alpha\beta}, \tag{A3c}$$

$$\sum_{\{ij\}} (\boldsymbol{\tau}_i + \boldsymbol{\tau}_j)_\alpha (\boldsymbol{\tau}_i + \boldsymbol{\tau}_j)_\beta = 16 \delta_{\alpha\beta}, \tag{A3d}$$

$$\sum_{\{ij\}} [\boldsymbol{\tau}_i \times \boldsymbol{\tau}_j]_\alpha [\boldsymbol{\tau}_i \times \boldsymbol{\tau}_j]_\beta = 32 \delta_{\alpha\beta}, \tag{A3e}$$

$$\sum_{\{ij\}} (\tau_{i\alpha} \tau_{j\beta} + \tau_{j\alpha} \tau_{i\beta}) = -8 \delta_{\alpha\beta}. \tag{A3f}$$

Using Eqs. (A3a)–(A3e) we can calculate the sums containing products of the vectors $\mathbf{b}_{n,ij}$, $\mathbf{D}_{n,ij}$ $(n = 1,2,3)$:

$$\sum_{\{ij\}} (\boldsymbol{\tau}_i - \boldsymbol{\tau}_j)_\alpha b_{1,ij\beta} = 4(-8x + 1) \delta_{\alpha\beta}, \tag{A4a}$$

$$\sum_{\{ij\}} (\boldsymbol{\tau}_i - \boldsymbol{\tau}_j)_\alpha b_{2,ij\beta} = 4(-8x + 3) \delta_{\alpha\beta}, \tag{A4b}$$

$$\sum_{\{ij\}} (\boldsymbol{\tau}_i - \boldsymbol{\tau}_j)_\alpha b_{3,ij\beta} = 4(-8x - 1) \delta_{\alpha\beta}, \tag{A4c}$$

$$\sum_{\{ij\}} (\boldsymbol{\tau}_i - \boldsymbol{\tau}_j)_\alpha D_{n,ij\beta} = 8 D_{n+} \delta_{\alpha\beta}, \tag{A5}$$

$$\sum_{\{ij\}} D_{n,ij\alpha} D_{n,ij\beta} = 4 D_n^2 \delta_{\alpha\beta}, \tag{A6}$$

$$\sum_{\{ij\}} b_{1,ij\alpha} b_{1,ij\beta} = (32x^2 - 8x + 2)\delta_{\alpha\beta}, \tag{A7a}$$

$$\sum_{\{ij\}} b_{2,ij\alpha} b_{2,ij\beta} = (32x^2 - 24x + 6)\delta_{\alpha\beta}, \tag{A7b}$$

$$\sum_{\{ij\}} b_{3,ij\alpha} b_{3,ij\beta} = (32x^2 + 8x + 2)\delta_{\alpha\beta}, \tag{A7c}$$

$$\sum_{\{ij\}} D_{1,ij\alpha} b_{1,ij\beta} = [(-8x + 1)D_{1+} - D_{1-} + 2D_{1y}]\delta_{\alpha\beta}, \tag{A8a}$$

$$\sum_{\{ij\}} D_{2,ij\alpha} b_{2,ij\beta} = [(-8x + 3)D_{2+} + D_{2-} + 2D_{2y}]\delta_{\alpha\beta}, \tag{A8b}$$

$$\sum_{\{ij\}} D_{3,ij\alpha} b_{3,ij\beta} = [(-8x - 1)D_{3+} + D_{3-} + 2D_{3y}]\delta_{\alpha\beta}. \tag{A8c}$$

*chizhikov@crys.ras.ru
†dmitrien@crys.ras.ru

[1] H. J. Williams, J. H. Wernick, R. C. Sherwood, and G. K. Wertheim, J. Appl. Phys. **37**, 1256 (1966).
[2] D. Shinoda and S. Asanabe, J. Phys. Soc. Japan **21**, 555 (1966).
[3] S. M. Stishov and A. E. Petrova, Phys. Usp. **54**, 1117 (2011).
[4] Y. Ishikawa, K. Tajima, D. Bloch, and M. Roth, Solid State Commun. **19**, 525 (1976).
[5] K. Motoya, H. Yasuoka, Y. Nakarnura, and J. H. Wernick, Solid State Commun. **19**, 529 (1976).
[6] U. K. Rößler, A. V. Bogdanov, and C. Pfleiderer, Nature (London) **442**, 797 (2006).
[7] S. V. Grigoriev, S. V. Maleyev, A. I. Okorokov, Yu. O. Chetverikov, P. Böni, R. Georgii, D. Lamago, H. Eckerlebe, and K. Pranzas, Phys. Rev. B **74**, 214414 (2006).
[8] W. Münzer, A. Neubauer, T. Adams, S. Mühlbauer, C. Franz, F. Jonietz, R. Georgii, P. Böni, B. Pedersen, M. Schmidt, A. Rosch, and C. Pfleiderer, Phys. Rev. B **81**, 041203 (2010).
[9] T. Adams, S. Mühlbauer, C. Pfleiderer, F. Jonietz, A. Bauer, A. Neubauer, R. Georgii, P. Böni, U. Keiderling, K. Everschor, M. Garst, and A. Rosch, Phys. Rev. Lett. **107**, 217206 (2011).
[10] S. D. Tewari, D. Belitz, and T. R. Kirkpatrick, Phys. Rev. Lett. **96**, 047207 (2006).
[11] B. Binz, A. Vishwanath, and V. Aji, Phys. Rev. Lett. **96**, 207202 (2006).
[12] A. Hamann, D. Lamago, Th. Wolf, H. v. Löhneysen, and D. Reznik, Phys. Rev. Lett. **107**, 037207 (2011).
[13] J. M. Hopkinson and H.-Y. Kee, Phys. Rev. B **74**, 224441 (2006).
[14] V. A. Chizhikov and V. E. Dmitrienko, Phys. Rev. B **85**, 014421 (2012).
[15] I. Dzyaloshinsky, Phys. Chem. Solids **4**, 241 (1958).
[16] P. Bak and M. H. Jensen, J. Phys. C: Solid State Phys. **13**, L881 (1980).
[17] O. Nakanishi, A. Yanase, A. Hasegawat, and M. Kataoka, Solid State Commun. **35**, 995 (1980).
[18] T. Moriya, Phys. Rev. **120**, 91 (1960).
[19] J. M. Hopkinson and H.-Y. Kee, Phys. Rev. B **79**, 014421 (2009).
[20] V. E. Dmitrienko and V. A. Chizhikov, Phys. Rev. Lett. **108**, 187203 (2012).
[21] S. Seki, X. Z. Yu, S. Ishiwata, and Y. Tokura, Science **336**, 198 (2012).
[22] T. Adams, A. Chacon, M. Wagner, A. Bauer, G. Brandl, B. Pedersen, H. Berger, P. Lemmens, and C. Pfleiderer, Phys. Rev. Lett. **108**, 237204 (2012).
[23] J. H. Yang, Z. L. Li, X. Z. Lu, M.-H. Whangbo, S.-H. Wei, X. G. Gong, and H. J. Xiang, Phys. Rev. Lett. **109**, 107203 (2012).
[24] A. K. Zvezdin and A. P. Pyatakov, Eur. Phys. Lett. **99**, 57003 (2012).
[25] S. A. Pikin and I. S. Lyubutin, Phys. Rev. B **86**, 064414 (2012).
[26] V. V. Mazurenko and V. I. Anisimov, Phys. Rev. B **71**, 184434 (2005).
[27] E. J. Samuelsen and G. Shirane, Phys. Status Solidi **42**, 241 (1970).
[28] M. Kenzelmann, A. B. Harris, S. Jonas, C. Broholm, J. Schefer, S. B. Kim, C. L. Zhang, S.-W. Cheong, O. P. Vajk, and J. W. Lynn, Phys. Rev. Lett. **95**, 087206 (2005).
[29] S.-W. Cheong and M. Mostovoy, Nat. Mater. **6**, 13 (2007).
[30] J. M. Hopkinson and H.-Y. Kee, Phys. Rev. B **75**, 064430 (2007).
[31] P. J. Brown, J. B. Forsyth, and G. H. Lander, J. Appl. Phys. **39**, 1331 (1968).
[32] A. S. Moskvin and I. G. Bostrem, Fiz. Tverd. Tela **19**, 1616 (1977) [Sov. Phys. Solid State **19**, 1532 (1977)].
[33] L. Shekhtman, A. Aharony, and O. Entin-Wohlman, Phys. Rev. B **47**, 174 (1993).
[34] I. A. Sergienko and E. Dagotto, Phys. Rev. B **73**, 094434 (2006).
[35] M. I. Katsnelson, Y. O. Kvashnin, V. V. Mazurenko, and A. I. Lichtenstein, Phys. Rev. B **82**, 100403 (2010).
[36] L. Shekhtman, O. Entin-Wohlman, and A. Aharony, Phys. Rev. Lett. **69**, 836 (1992).
[37] T. Yildirim, A. B. Harris, A. Aharony, and O. Entin-Wohlman, Phys. Rev. B **52**, 10239 (1995).
[38] T. Hahn (ed.), *International Tables for Crystallography, Vol. A: Space-Group Symmetry* (Kluwer Academic, Dordrecht, 1989).
[39] V. Dmitriev, D. Chernyshov, S. Grigoriev, and V. Dyadkin, J. Phys.: Condens. Matter **24**, 366005 (2012).
[40] X. Z. Yu, Y. Onose, N. Kanazawa, J. H. Park, J. H. Han, Y. Matsui, N. Nagaosa, and Y. Tokura, Nature (London) **465**, 901 (2010).
[41] X. Z. Yu, N. Kanazawa, Y. Onose, K. Kimoto, W. Z. Zhang, S. Ishiwata, Y. Matsui, and Y. Tokura, Nat. Mater. **10**, 106 (2011).
[42] F. Keffer, Phys. Rev. **126**, 896 (1962).
[43] M. A. Ruderman and C. Kittel, Phys. Rev. **96**, 99 (1954).
[44] T. Kasuya, Prog. Theor. Phys. **16**, 45 (1956).
[45] K. Yosida, Phys. Rev. **106**, 893 (1957).
[46] J. H. Van Vleck, Rev. Mod. Phys. **34**, 681 (1962).
[47] T. R. Kirkpatrick and D. Belitz, Phys. Rev. B **80**, 220401(R) (2009).
[48] A. Gukasov and P. J. Brown, J. Phys.: Condens. Matter **14**, 8831 (2002).
[49] H. Cao, A. Gukasov, I. Mirebeau, P. Bonville, C. Decorse, and G. Dhalenne, Phys. Rev. Lett. **103**, 056402 (2009).
[50] U. K. Rößler, A. A. Leonov, and A. V. Bogdanov, J. Phys.: Conf. Ser. **303**, 012105 (2011).

[51] S. V. Grigoriev, D. Chernyshov, V. A. Dyadkin, V. Dmitriev, S. V. Maleyev, E. V. Moskvin, D. Menzel, J. Schoenes, and H. Eckerlebe, Phys. Rev. Lett. **102**, 037204 (2009).

[52] S. V. Grigoriev, N. M. Potapova, S.-A. Siegfried, V. A. Dyadkin, E. V. Moskvin, V. Dmitriev, D. Menzel, C. D. Dewhurst, D. Chernyshov, R. A. Sadykov, L. N. Fomicheva, and A. V. Tsvyashchenko, Phys. Rev. Lett. **110**, 207201 (2013).

[53] K. Shibata, X. Z. Yu, T. Hara, D. Morikawa, N. Kanazawa, K. Kimoto, S. Ishiwata, Y. Matsui, and Y. Tokura, Nat. Nanotechnol. **8**, 723 (2013).